Effects of electron-phonon coupling and electron diffusion on ripples growth on ultrafast-laser-irradiated metals

Jean-Philippe Colombier, Florence Garrelie, Nicolas Faure, Stéphanie Reynaud, Mourad Bounhalli, Eric Audouard, Razvan Stoian, Florent Pigeon

Effects of electron-phonon coupling and electron diffusion on ripples growth on ultrafast-laser-irradiated metals

J. P. Colombier, F. Garrelie, N. Faure, S. Reynaud, M. Bounhalli et al.

Citation: J. Appl. Phys. **111**, 024902 (2012); doi: 10.1063/1.3676221
View online: http://dx.doi.org/10.1063/1.3676221
View Table of Contents: http://jap.aip.org/resource/1/JAPIAU/v111/i2
Published by the American Institute of Physics.

Effects of electron-phonon coupling and electron diffusion on ripples growth on ultrafast-laser-irradiated metals

J. P. Colombier,[a] F. Garrelie, N. Faure, S. Reynaud, M. Bounhalli, E. Audouard, R. Stoian, and F. Pigeon
Université de Lyon, Laboratoire Hubert Curien, UMR 5516 CNRS, Université Jean Monnet, 42000 Saint-Etienne, France

(Received 19 July 2011; accepted 7 December 2011; published online 17 January 2012)

Metals exposed to ultrafast laser irradiation close to ablative regimes show often a submicron-scale (near 0.5 μm) periodic organization of the surface as ripples. Using two classes of metallic materials (transition and noble), we have determined that the ripples amplitude is strongly correlated to the material transport properties, namely electron-phonon relaxation strength, electronic diffusion, and to the energy band characteristics of the electronic laser excitation. This particularly depends on the topology of the electronic structure, including *d*-band effects on electronic excitation. Comparing the effects of electron-phonon nonequilibrium lifetimes for the different metals under similar irradiation conditions, we indicate how the electron-phonon coupling strength affects the electronic thermal diffusion, the speed of phase transformation and impacts on the ripples contrast. The highest contrast is observed for ruthenium, where the electron-phonon coupling is the strongest, followed by tungsten, nickel, and copper, the latter with the least visible contrast. The dependence of surface patterns contrast with fluence is linked to the dependence of the relaxation characteristics with the electronic temperature. © *2012 American Institute of Physics*. [doi:10.1063/1.3676221]

I. INTRODUCTION

Laser induced periodic surface structures (LIPSS), a periodic nanoscale arrangement also called ripples, have been observed substantially near the ablation threshold on metallic surfaces.[1–5] In the most common type of surface topography, a periodicity of about the wavelength λ of the laser radiation is noted. The great variety of experimental LIPSS was described with different physical approaches, being typically attributed to the interference between the incident laser radiation and scattered or excited surface waves.[6,7] Higher frequency patterns were also observed,[8] and interpreted as a consequence of second and higher harmonics generation at the surface even if the exact formation mechanism remains an open question. Because of the wide range of LIPSS, additional physical approaches have also been considered, in particular effects resulting from field enhancement by nanorugosity, surface stress, inhomogeneous deposited energy distribution, or frozen capillary waves. In the case of metals, ripples are found to grow along the direction perpendicular to the laser polarization, even if high spatial frequency LIPSS parallel to the incident electric field have been reported.[9] A possible plasmonic nature of ripples generation has been indicated in various works,[10,11] with a recent contribution supporting the correlation between ripples formation under ultrashort laser exposure and surface plasmons (SP) generation conditions.[11] Additionally, repeating laser pulses induce cumulative phenomena, resulting in subsequent ripples growth at varying periodicities via a positive feedback process. Modulation of the energy interaction could also depend on a spatial variation of the dielectric constants, which could modify the electric field distribution.[12] The question of the initial conditions required for the ripples formation is therefore complex, especially since the launching mechanisms are not yet accessible to observations. For instance, it is not known if the periodicity of these structures is a consequence of laser light modulations at the beginning of the interaction, due to some instabilities occurring during the liquid phase and frozen by the resolidification,[13] or an association of these two processes. To decide which mechanisms are effective during ripples formation and to establish a suitable scenario, one possibility is to compare experimental conditions and materials with different intrinsic properties and to deduce how metal features could impact on the end results.

Previous studies have shown that ripples on metallic surfaces are affected by the competition of two ultrafast processes, electron-phonon energy coupling and hot electron diffusion. However, these investigations were limited to the case of noble metals.[3,4,14] We extend the comparison for two classes of metals, particularly transition and noble, with largely different physical and thermodynamic properties, and differing tendencies for ripples formation. These are investigated here to provide more insights into the relation between material properties and LIPSS. The nature and intensity of the laser-metal interaction and the relaxation of the energy inside the material are clearly shown to be of importance when discussing the mechanism for periodic nanostructures formation. In particular, the electron-phonon coupling strength γ, varying at least on one order of magnitude depending on the metal, limits the electronic thermal diffusion deeper into the bulk and impacts

[a]Authors to whom correspondence should be addressed. Electronic addresses: Jean.Philippe.Colombier@univ-st-etienne.fr and Florence.Garrelie@univ-st-etienne.fr.

the dimensional regions affected by phase transitions. In this work, the relative strength and the electron temperature dependence of the electron-phonon coupling in the metals are identified as key factors affecting the initial energy redistribution and the location of the region undergoing transient melting and subsequent growth before resolidification, contributing to define the ripples contrast.

II. EXPERIMENTAL PROCEDURES

The laser system used in the experiment is an amplified Ti:sapphire laser with a pulse duration of 150 fs full width at half-maximum (FWHM) at a repetition rate of 1 kHz and a wavelength of 800 nm. The number of pulses used for the sample irradiation is fixed to 50 using a Pockels cell control unit. The laser beam is horizontally polarized and is focused at normal incidence, through an achromatic lens of 50.8 mm focal length, onto a metal sample mounted on an X-Y-Z motorized translation stage. The different materials used in this study are ruthenium, tungsten, nickel, and copper. All the samples are placed at the image point of an aperture (diameter 2.8 mm) situated in the beam path. A truncated Gaussian, smeared by diffraction effects is thus projected at the image plane. This can be roughly assumed to be a Gaussian beam with a dimension (at $1/e^2$ intensity) determined by the classical linear regression of the impact surface versus the energy logarithm.[15] The on target delivered power is finely controlled by a half-wave plate-polarizer pair. The structuring of the samples is conducted in air. Analysis of the modification of the surfaces under the action of the femtosecond light pulses is performed using a scanning electron microscope (FEI, NovaNanoSEM). The topography of surface structures is studied in the acoustic ac mode of an atomic force microscope (AFM) (Agilent 5500), which is a resonant mode, equivalent to tapping mode of Veeco's AFM.

III. RESULTS

Irradiation of metal samples at a pulse energy of 30 μJ induces ripples on all materials as indicated in Fig. 1(a) for Ru, W, Ni, and Cu. The ripples are observed to be perpendicular to

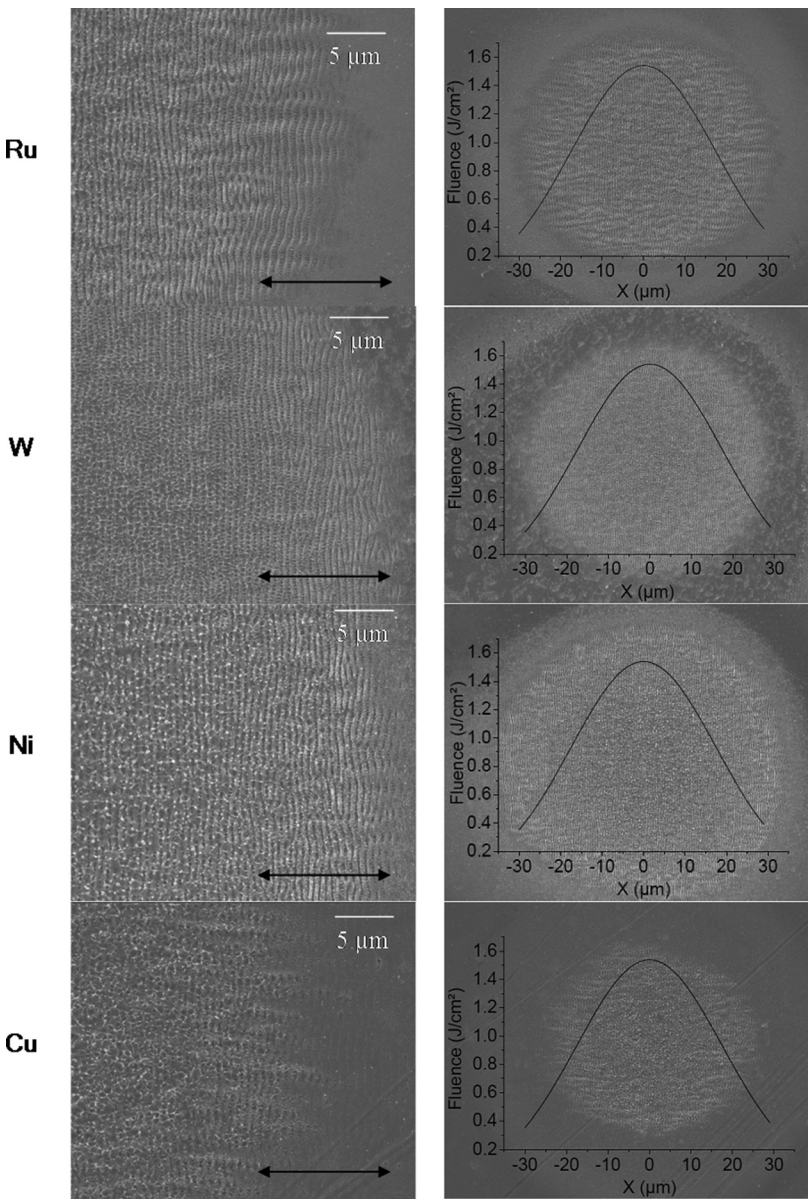

FIG. 1. Surface ripples induced by N = 50 laser pulses of 150 fs delivering an energy of 30 μJ/pulse (averaged laser fluence of 0.77 J/cm^2), on Ru, W, Ni, and Cu: (a) SEM images. The electric field direction is indicated by the arrow. (b) Gaussian fit profile of the laser beam intensity, as determined from the beam waist measurement.

the incident electric field indicated as an arrow in Fig. 1, consistently with a surface plasmon wave excitation interacting with the laser. Here, very regular patterns are formed within the laser spot. The presence of a liquid phase during the formation of the ripples is perceptible from the observation of small ejections around the impact area. The Gaussian laser beam profile superimposed on the laser impact (Fig. 1(b)) shows obviously that the energy of the laser pulse is significantly higher in the center of the irradiated area. Consequently, the outer regions of the laser impact are irradiated only with the lower energy edges of the pulses. The diameter of the beam is determined to be about 70 μm, allowing to estimate the local fluence and its distribution inside the laser impact. As a result, SEM images (Fig. 1) provide a qualitative view of the surface relief, and a more detailed topography analysis is performed by AFM analysis (Fig. 2). The spacing of the ripples is determined from both SEM and AFM, and it is found to be approximately 600 nm for all the materials. All metallic surfaces have been irradiated at a fixed input laser energy. The ripples amplitude measured by AFM is given in Fig. 2(b) and indicate that material characteristics play a fundamental role. The amplitude of the ripples varies as a function of the material, as previously

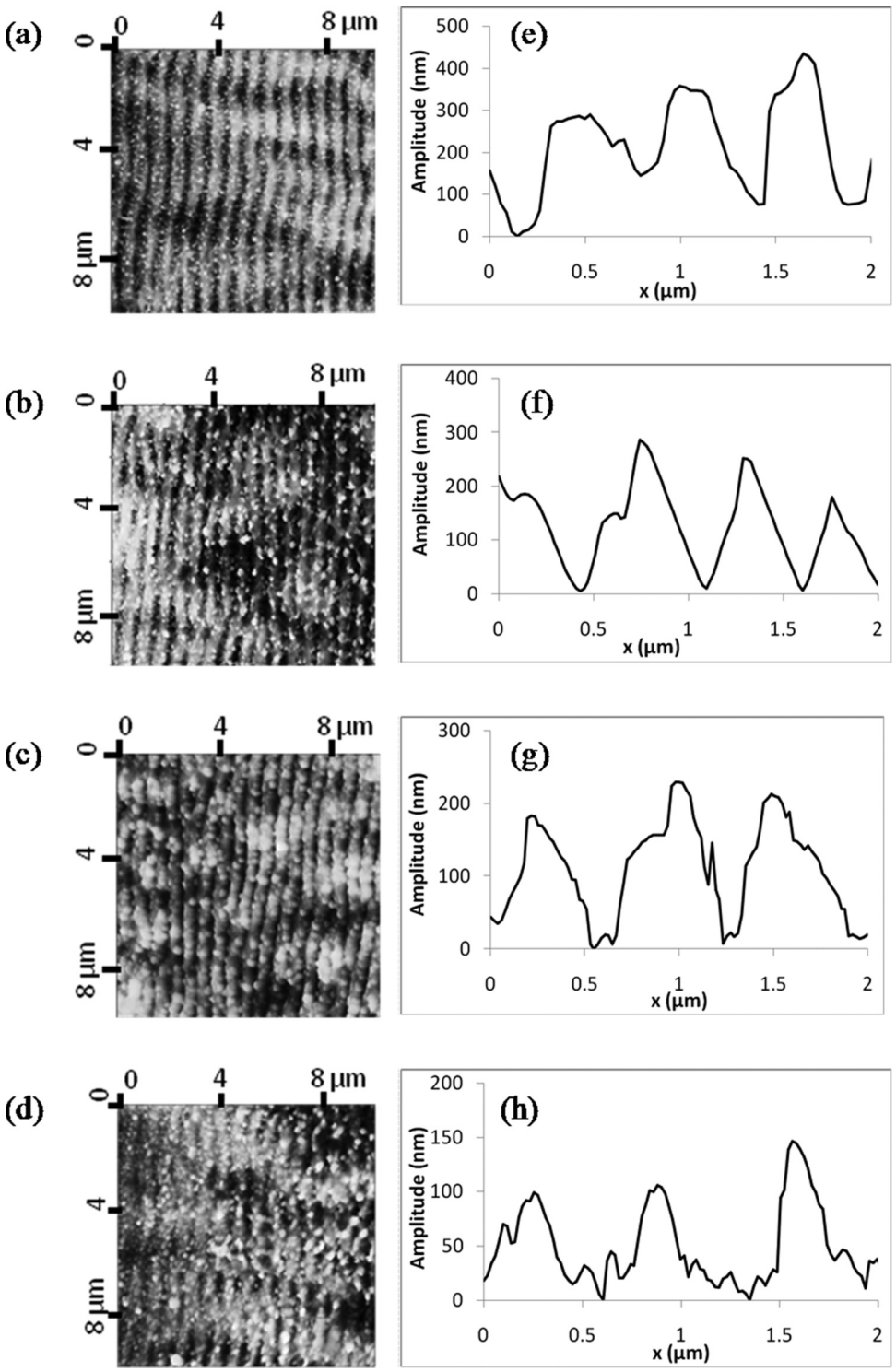

FIG. 2. Analysis of ripples morphology on the different materials employed: Ru (a,e), W(b,f), Ni(c,g), and Cu (d,h). AFM images on 10 μm × 10 μm areas (a,b,c,d) and typical profile lines from AFM images, showing the cross-section of the ripples topography at local fluence around 0.6 J/cm^2 (e,f,g,h).

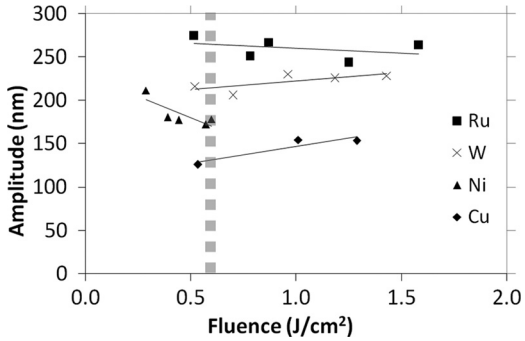

FIG. 3. Height of the averaged cross-section of the surface ripples obtained for different materials with N = 50 pulses as a function of the local fluence in the spot. The dashed line indicates the fluence values corresponding to AFM measurements in Fig. 2. Solid lines guide the eye.

indicated in works on noble metals.[3,4] The amplitude of the ripples, measured at various values of local fluence within the impact region is reported on Fig. 3. It has to be noted that the highest fluence values correspond to a regime where ablation occurs in the center of the spot perturbing the pattern, which is not contradictory with ripples formation at the edge.[16] The behavior of ripples with the fluence is rather complex. It appears that ripples amplitude does not vary with the local fluence in the same way for all materials. As ripples are supposed to appear only when a sufficient energy is deposited at the surface to induce liquid phase transformation and material flow, a fluence threshold is expected. Additionally, higher fluence should preferentially produce vaporization and ablation of the surface, losing the modulated energy deposition and preventing periodic nanostructures formation. Consequently, an intermediate regime allowing ripples formation is expected. However, a well-defined maximal amplitude for a given fluence does not appear as shown on Fig. 3 for the measurable fluence range (high signal to noise ratio) and different materials show different tendencies with a monotonous character.

We discuss below particular fluence ranges. At a local fluence of 0.5 J/cm^2, the amplitude of ripples depends on materials and allows a ranking of materials in the following order: Ruthenium, tungsten, nickel, and then finally copper. This matches exactly the ranking of materials based on the γ values, and the absorptivity A of these materials. A, γ values for $T_e = 5000$ K, thermal conductivity κ, penetration depth δ are reported for comparison in Table I. Ruthenium has been chosen for the high expected A and γ values.[17] The other materials were selected because of their different electronic structure and antagonic behavior of γ with electronic temperature T_e that either increases or decreases at increasing T_e.[18] Absorptivity and electron-phonon coupling strength are both relatable to the electron energy loss by electron and phonon scattering. This way, the strength of electron-phonon coupling is equivalent to the efficiency of localizing energy and justifies the observed correlation. The nature of this localization is collisional. For this reason, other material properties dependent on such scattering rate, defining also the rate and the profile of the energy deposition, as surface plasmon damping, are supposed to follow a similar ranking. The end profile defines the energy confinement and the subsequent morphological characteristics of the metal surface as reported by Huang *et al.*[10] To extend this observation, the optical penetration depth δ is also provided in Table I**,** since the decay length of electromagnetic waves inside the material should influence the modification size at the surface. As the optical penetration depth of tungsten is higher than those of the other materials examined here, the resulting electromagnetic confinement is the lowest. However, in view of their larger scale, the different confinements in these materials are rather attributed to relaxation phenomena occurring later after irradiation, as discussed in the next section. The ripples contrast we observe is in the range of several hundred nanometers. A second observation can be made regarding the evolution of ripples contrast with fluence from Fig. 3. We observe that it does not follow the same monotonous behavior for all materials. We will show below that this behavior follows also the evolution of the strength of the electron-phonon coupling γ with laser excitation. From *ab initio* calculations, Lin *et al.*[18] have shown a γ increase or decrease with electronic temperature, for different metals under strong electron-phonon nonequilibrium. Our results indicate an increase of the ripples amplitude with the increasing fluence, for Cu and W, while Ni exhibits a significant decrease and Ru decreases softly. The evolutions for these materials follow the evolution of the electron-phonon strength γ with temperature.[18] As a result, the electronic dynamics subsequent to laser heating and dependent on laser fluence could be a driving factor for the nanostructures growth, particularly in their spatial extension. This extrapolation concerns fast change in electron-phonon coupling that may transiently change the coupling conditions of the target material. It yields, in turn, the reduction of the thermally affected layer thickness as detailed in the next section.

IV. DISCUSSION

This section proposes a discussion on the basis of some characteristics of these different materials under ultrashort pulse irradiation, relevant for explaining the observed

TABLE I. Material properties for metals investigated (Refs. 29 and 30): absorptivity A, penetration depth δ, thermal conductivity κ, electron-phonon coupling strength γ, melting temperature T_m, and ion heat capacity C_i. γ values have been taken from Ref. 18 for W, Ni, Cu, and from Ref. 17 for Ru.

Metals	A (%)	δ (nm)	K (W.m^{-1}.K^{-1})	$\gamma \times 10^{17}$ (W.m^{-3}.K^{-1}) (at $T_e = 5000$ K)	T_m (K)	C_i (x10^6 J.K^{-1}.m^{-3})
Ru	61.2	16.2	117	18.5 (300 K)	2607	2.94
W	50.4	23.3	170	4.3	3695	2.61
Ni	31.7	14.5	91	2	1728	3.79
Cu	3.7	12.6	398	2.1	1358	3.53

behaviors. Interaction of an ultrashort laser pulse with metal surface leads to a rapid increase in electronic temperature T_e, whereas the thermalization between electron and ion subsystems occurs on a substantially longer time-scale (approximately 1–50 ps).[19] Consequently, significant changes in the absorption of the visible and infrared light in metallic surfaces occur along the optical penetration depth. At laser intensities close to ablation threshold (around 10^{12}–10^{13} W/cm^2), T_e typically reaches 10^4 K at surface and a significant redistribution occurs between the electron energy states, while ions remain essentially cold. The dynamics reveals a three-step process that is associated with the (1) complex laser light absorption, (2) nonequilibrium with extremely localized electronic temperatures in short timescales, and (3) hydrodynamic relaxation processes that cool down the surface of the metallic system and could generate instabilities of the moving gas-liquid or liquid-solid contact lines.

At nanometer scales defined by δ values, the free-space impinging light is coupled to surface electromagnetic modes to give rise to surface plasmon modes, in particular conditions related to optical properties met on short time scales.[11] As discussed below, the laser excitation affects the evolution of the density of the *d* and *s*/*p* states. Consequently, the number of free electrons and the electron collision frequency can change drastically and the optical properties evolve significantly.[11,19] Moreover, it is interesting to note that even if tungsten has a positive real part of dielectric constant in standard conditions, which prevents SP propagation at a metal/air interface, ripples have been observed in the present experiment and also reported and discussed by other authors in Ref. 20 where the transient variation of the dielectric function seems possible. A strong electrical field occurs at the metal surface corresponding to a SP generation along the metal-air interface in addition to the radiation. Along with the interference hypothesis corresponding to the laser-SP interaction,[21] the surface areas heated by the maxima of the field intensity could experience a higher coupling of energy than those heated by the minima, causing a modulated energy deposition and a large temperature gradient from the ridge to the valley of a pre-ripple.

We will approach the conditions of ripples formation from a perspective that regards the dimensional region affected by radiation. The duration of thermal relaxation is determined by the rate of energy exchange between electrons and the lattice. In the first moments, which lasts a few picoseconds, the electron and phonon systems begin to equilibrate, and a thin surface layer undergoes melting. During this stage, electronic heat conduction away from the excited region is limited by the (e-ph) relaxation time that is shorter if electron scattering from *d*-band excitations occurs. This impacts severely the size of the liquid region, with a first effect related to the observed fluence influence. To investigate the correlation between the electronic structure dynamics subsequent to laser heating and the nanostructure feature dependence on laser fluence, the estimated electron diffusion depth L_c has been compared to the ripples amplitude. L_c is related to the expected molten layer[22] and depends on the T_e longitudinal profile reached at the complete relaxation time that is directly relating to the electron mean free path as $L_c \propto \lambda_e$. The dependence of the layer thickness L_c can be estimated by[23]

$$L_c = \left(\frac{128}{\pi}\right)^{1/8} \left(\frac{C_i}{A_e T_m}\right)^{1/4} \left(\frac{K}{\gamma}\right)^{1/2} \quad (1)$$

relating the electronic diffusion length to the melt temperature T_m, and the (e-ph) coupling strength γ. A_e represents the linear dependence in T_e of the electron heat capacity, and C_i is the ion heat capacity.

The L_c dependence on T_e, reported in Fig. 4, has been calculated to emphasize the evolution of the energy confinement size as a function of an effective electronic temperature, with respect to the fluence dependent experimental results. The effective penetration depth of hot electrons L_c, characterizing the extent of inner energy redistribution during (e-ph) equilibration at the threshold for melting, is useful to estimate qualitatively the laser-induced energy confinement. In this rough estimation, it is assumed that the ripples formation is restrained to a melting phase at the metal surface with a temperature close to the melting one and that a fluence augmentation in the experiment is directly connected to a higher average T_e. For Cu and W, when the electronic temperature is increased, λ_e drops and L_c decreases. An inverse process occurs for Ni, which could explain the change in metal arrangement observed in Fig. 3. This counterintuitive result can be interpreted in terms of the electronic structure topology. The band structure of Cu consists on a broad, nearly free-electron-like *s*-*p* band, located several eV below the Fermi energy, which overlaps and hybridizes with a relatively thin *d*-band (at 3.5 eV), easy to excite. For Cu, as other noble metals, a large number of *d* electrons are thermally excited when T_e increases, yielding a high strengthening of the electron-phonon coupling γ. This induces a reduction of the electron mean free path $\lambda_e \approx \upsilon_F \tau_{ep}$, where υ_F is the Fermi electron velocity and τ_{ep} the (e-ph) characteristic time. The tendency is reversed for transition metals 3 d (Ni), 4 d (Ru) and also for 5 d (W) at higher T_e [not visible on Fig. 4 for W]. These transition metals are different from Cu due to the Fermi level that falls in the *d*-band while in the noble metal, the *d*-bands are full. In the case of excited transition metals, the thermal excitation of *d*-band electrons from

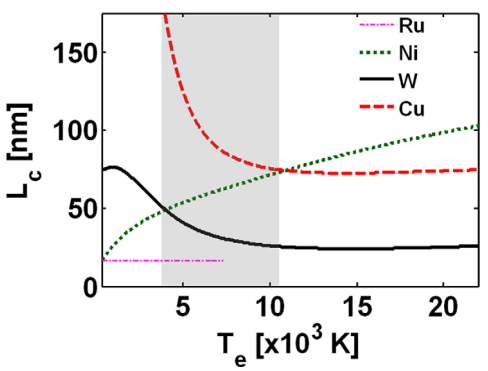

FIG. 4. (Color online): Calculated electronic temperature dependence of the electron diffusion depth (L_c) in the various solid materials at the melting threshold. The window corresponding to the expected range of ripples formation is represented by the gray area.

below the Fermi level to higher energy states shifts the chemical potential.[24] The energy distribution is modified and γ decreases as T_e increases. The contribution to the electron-phonon coupling γ from *d*-band electrons is then reduced when T_e increases. The evolution of the electron-phonon strength γ of Ru with temperature is not available in the literature, but results obtained in the present work suggest a soft decrease of γ with electronic temperature for this metal. This effect has been shown by Ref. 18 for Ni and Ti but similar arguments should remain valid for Ru. For W, due to high density of *d*-states on both sides of the Fermi level the γ decrease starts for T_e higher than the considered range[25] and L_c shows a slight decrease on Fig. 4 for this metal. The energy confinement size can be related to the molten layer experiencing the subsequent longitudinal gradient of metal temperature $\bigtriangledown_z T$. This gradient determines the pressure distribution and drives the expansion perpendicular to the surface at the sound velocity. A rapid *e-ph* relaxation will induce a first inertial stress confinement conditioning a high initial momentum inducing a hydrodynamic flow.[26,27] The surface gradients could also involve local Marangoni force, which can affect the ripples growth.[14,28] Both thermal diffusion and hydrodynamical motion cool down the molten layer that undergoes solidification, freezing the metal surface. The liquid-solid interface advances toward the surface and results in a resolidified layer a few tens of nanometers in thickness. The kinetics of the transient melting and resolidification, occurring under conditions of the fast cooling due to the two-dimensional electron heat conduction, could define the shape of the surface topography.

V. CONCLUSION

The present study is focused on the role of electron-phonon coupling in ripples formation on metallic materials under ultrafast laser irradiation. The main conclusions may be highlighted as followed:

- The relative amplitudes of the surface patterns on ruthenium, tungsten, nickel, and copper match the ranking of these materials based on the (e-ph) coupling strength and the absorptivity.
- Electron-phonon coupling strength is a key parameter influencing the ripples growth on metals.
- The amplitude of the ripples, measured at various values of the fluence, is well supporting the expected evolution of the strength of the electron-phonon coupling with temperature via the energy confinement in an emerging liquid layer.
- Ruthenium for which the evolution of electron-phonon coupling with temperature was unknown seems to have a similar behavior as nickel, with a soft decrease of ripples contrast with fluence.
- Metals with electronic properties allowing a strong confinement of the energy are more susceptible to ripples growth. When the (e-ph) coupling strength is high, a thin layer is molten, and ripples growth is expected due to strong temperature gradients.

[1]M. Birnbaum, J. Appl. Phys. **36**, 3688 (1965).
[2]D. C. Emmony, R. P. Howson, and L. J. Willis, Appl. Phys. Lett. **23**, 598 (1973).
[3]J. Wang and C. Guo, Appl. Phys. Lett. **87**, 251914 (2005).
[4]J. Wang and C. Guo, J. Appl. Phys. **100**, 023511 (2006).
[5]S. Sakabe, M. Hashida, S. Tokita, S. Namba, and K. Okamuro, Phys. Rev. B **79**, 033409 (2009).
[6]D. J. E. Sipe, J. F. Young, J. S. Preston, and H. M. van Driel, Phys. Rev. B **27**, 1141 (1983).
[7]Z. Guosheng, P. M. Fauchet, and A. E. Siegman, Phys. Rev. B **26**, 5366 (1982).
[8]A. Borowiec and H. K. Haugen, Appl. Phys. Lett. **82**, 4462 (2003).
[9]J. Bonse, M. Munz, and H. Sturm, J. Appl. Phys. **97**, 013538 (2005).
[10]M. Huang, F. Zhao, Y. Cheng, N. Xu, and Z. Xu, ACS Nano **3**, 4062 (2009).
[11]F. Garrelie, J. P. Colombier, F. Pigeon, S. Tonchev, N. Faure, M. Bounhalli, S. Reynaud, and O. Parriaux, Opt. Express **19**, 9035 (2011).
[12]M. Huang, F. Zhao, Y. Cheng, N. Xu, and Z. Xu, Phys. Rev. B **79** 125436 (2009).
[13]J. Reif, F. Costache, O. Varlamova, G. Jia, and M. Ratzke, Phys. Status Solidi C **6**, 681 (2009).
[14]T. Y. Hwang, A. Y. Vorobyev, and C. Guo, Appl. Phys. Lett. **95**, 123111 (2009).
[15]J. M. Liu, Opt. Lett. **7**, 196 (1982).
[16]K. Okamuro, M. Hashida, Y. Miyasaka, Y. Ikuta, S. Tokita, and S. Sakabe, Phys. Rev. B **82**, 165417 (2010).
[17]M. Bonn, D. N. Denzler, S. Funk, and M. Wolf, Phys. Rev. B **61**, 1101 (2000).
[18]Z. Lin, L. V. Zhigilei, and V. Celli, Phys. Rev. B **77**, 075133 (2008).
[19]S. I. Anisimov, B. L. Kapeliovich, and T. L. Perel'man, Sov. Phys. JETP **39**, 375 (1974).
[20]A. Y. Vorobyev and C. Guo, J. Appl. Phys. **104**, 063523 (2008).
[21]V. S. Makin, R. S. Makin, A. Y. Vorobyev, and C. Guo, Tech. Phys. Lett. **34**, 387 (2008).
[22]S.-S. Wellershoff, J. Hohlfeld, J. Güdde, and E. Matthias, Appl. Phys. A **69**, S99 (1999).
[23]P. B. Corkum, F. Brunel, N. K. Sherman, and T. Srinivasan-Rao, Phys. Rev. Lett. **61**, 2886 (1988).
[24]P. E. Hopkins, J. M. Klopf, and P. M. Norris, Appl. Opt. **46**, 2076 (2007).
[25]For more information on electron-phonon coupling evolution: see http://www.faculty.virginia.edu/CompMat/electron-phonon-coupling/.
[26]J. P. Colombier, P. Combis, F. Bonneau, R. Le Harzic, and E. Audouard, Phys. Rev. B **71**, 165406 (2005).
[27]D. S. Ivanov, Z. Lin, B. Rethfeld, G. M. O'Connor, T. J. Glynn, and L. V. Zhigilei, J. Appl. Phys. **107**, 013519 (2010).
[28]M. Gedvilas, B. Voisiat, G. Raciukaitis, and K. Regelskis, Appl. Surf. Sci. **255**, 9826 (2009).
[29]*Handbook of Optical Constants of Solids*, edited by E. D. Palik (Academic, New York, 1985).
[30]Note that the absorptivity of a metal surface can be strongly dependent on the surface roughness. In particular, for Cu, Ref. 3 indicates an absorptivity four times higher ($A \approx 13\%$) than A given by Ref. 29.